Iranian Journal of Medical Physics

ijmp.mums.ac.ir

Development and Validation of a TPS-Derived Feature Based Predictive Model for Adaptive Radiotherapy Support: APE-Net

Daniel Warurii Ndegwa[1*], Martin Mule Mutie[2], Paul Kuria Kamweru[3], James Ngure [4]

1. Daniel Warurii Ndegwa, Department of Physical Sciences, Chuka University, Kenya.
2. Martin Mule Mutie, Department of Physical Sciences, Chuka University, Kenya.
3. Paul Kuria Kamweru, Department of Physical Sciences, Chuka University, Kenya.
4. James Ngure, Senior Consultant Medical Physicist-Radiation Oncology, M.Sc, Kenya.

ARTICLE INFO

Article type:
Original Paper

Keywords:
Head and Neck Cancer (HNC)
Limited-Resource Setting
Synthetic TPS-Derived Feature
Predictive Modelling
Anatomical Changes

ABSTRACT

Introduction: Radiotherapy for advanced head and neck cancer (HNC) is complicated by anatomical changes, tumor shrinkage, and organ displacement, which may cause dosimetric inaccuracies and increased toxicity. Adaptive radiotherapy (ART) remains challenging in resource-limited settings due to time and personnel constraints. This study investigated the feasibility of the Anatomy-Preserving Estimation Network (APE-Net), a treatment planning system (TPS)-informed predictive framework for supporting offline adaptive radiotherapy (oART).

Material and Methods: Data from 21 retrospectively analyzed HNC patients were used, including baseline (Plan 1), unadapted (Plan 2), and adapted (Plan 3) treatment plans. Patients underwent cone-beam computed tomography (CBCT) monitoring, with rescan CT (rCT) acquired when anatomical deviations of >1 cm occurred. Plan 2 was recalculated using rCT images and original treatment parameters, while Plan 3 was re-optimized using the Eclipse TPS (Version 16, Varian Medical Systems, Palo Alto, CA, USA) at Moi Teaching and Referral Hospital, Eldoret, Kenya. TPS-derived dosimetric and volumetric features were extracted. 108 synthetic TPS-derived feature samples for augmentation were generated. APE-Net was implemented as a fully connected multilayer perceptron (MLP) trained on TPS-derived feature vectors to estimate adaptive treatment parameters.

Results: APE-Net trained on both real and synthetic TPS-derived features demonstrated moderate predictive performance, achieving a coefficient of determination (R^2) of 0.681, mean absolute error (MAE) of 9.092% and root mean squared error (RMSE) of 16.776%. Training and validation loss curves showed stable convergence with limited divergence.

Conclusion: APE-Net demonstrates feasibility as a TPS-informed machine-learning framework for supporting predictive oART workflows in resource-limited settings.

► *Please cite this article as:*
Ndegwa DW, Mutie MM, Kamweru PK, Ngure J. Development and Validation of a TPS-Derived Feature Based Predictive Model for Adaptive Radiotherapy Support: APE-Net. Iran J Med Phys 2026; 23 (2): 111-116. 10.22038/ijmp.2026.95287.2688.

Introduction

Adaptive radiation therapy matches the treatment plan to account for anatomical changes in the patient's anatomy during radiation therapy [1]. During head and neck tumor (HNC) therapy, radiographers mainly rely on visual observation to determine offline changes to the thermoplastic mask and subsequent re-planning [2]. Tumor changes and nodal reduction can be observed using cone beam computed tomography (CBCT) imaging, which helps to make clinical decisions about the impact of treatment changes [3]. In settings where clinical specialists in radiotherapy units such as medical physicists, radiation therapists and radiation oncologists are limited and treatment planning throughput is strained, predictive models have the potential to provide a scalable, interpretable bridge towards ART implementation [4].

Time and human resource constraints are the main limitations of ART. This means that treatment plans are rarely modified during the treatment course despite the internal changes of the patient [5]. Anatomical changes contribute to errors in dose placement, sub-optimal disease responses and radiation induced toxicities [6]. ART serves to address patient-specific treatment variations of systematic anatomical changes (weight, tumor and organ geometry), and biological response. It covers for stochastic variations such as organ deformation, filling change, respiration and peristaltic motion that appear on different time scales over the course of treatment schedules [7].

Offline adaptive radiotherapy (oART) improves the precision and efficiency of radiotherapy while minimizing radiation toxicity to the neighboring healthy organs [6]. The achievability of oART in limited resource settings calls for computational methods of ART [4]. Anatomy-Preserving Estimation Network (APE-Net), a deep learning model, was developed and implemented to support oART decision

*Corresponding Author: Tel: +254708396010; Email: danielwarurii1@gmail.com

making for advanced HNC. It was implemented as a fully connected multilayer perceptron (MLP) trained on TPS-derived tabular dosimetric and volumetric scalar feature vectors extracted from contoured CT/CBCT-guided adaptive workflows, rather than raw 3D anatomical image tensors or voxel-level spatial dose matrices. Predictive performance was evaluated using TPS-derived adaptive dosimetric and volumetric parameter estimation tasks [8].

Materials and Methods

The retrospective cohort consisted of 21 adult male and female patients aged above 21 years with advanced stage III and IV head-and-neck cancer undergoing concurrent chemo-radiotherapy. In the available dataset, the observed patient age range was 21–45 years. Ethical approval for the use of retrospective patient data was obtained from Moi Teaching and Referral Hospital/Moi University Institutional Scientific and Ethical Review Committee (MTRH/MU-ISERC) under approval number 0005091 and Chuka University Institutional Ethics Review Committee (CUIERC) under reference number CUIERC/NACOSTI/830. Research authorization was further granted by the National Commission for Science, Technology and Innovation (NACOSTI), Kenya, under research license number NACOSTI/P/25/4177302 and reference number 355200.

Patients received concurrent chemo-radiotherapy, with daily radiation dose of 2 Gy for 33 fractions, and treatment was carried using the sequential boost VMAT technique. Each patient had three treatment plans prepared: original plan (plan 1), unadapted plan (plan 2) and adapted plan (plan 3). For each plan, the dosimetric features were recorded that included the size of clinical target volume (CTV), the dose (maximum, minimum and mean), mean doses to organs at risk (OAR): left and right parotid gland and oral cavity, conformity index, gradient measure and gamma pass-rate. Adaptive re-planning was triggered by interim imaging, CBCT, on the n^{th} fraction or fractions after in radiation treatment, when anatomical deviations of >1 cm occurred on the CBCT capture. CBCTs were acquired during the first three fractions and weekly during RT. The differences between the CBCT images for the first day and the other treatment days were recognized as anatomical changes and visualized to recognize the location. A comparison of the difference in the lateral neck distance (△LND) on the corresponding CBCT images was performed. Rescan CT (rCT) was acquired when anatomical deviations of >1 cm occurred on the CBCT capture. The VMAT plans on the rCT images were compared to the original plans on the planning CT (pCT) using the dosimetric parameters for the target and the OAR, with plan evaluations from the both plans' dose volume histograms (DVH).

To evaluate the impact of anatomical changes on dose distribution, rCT was conducted and a treatment plan regenerated. The CTV and OAR were recontoured using CBCT and rCT images. All treatment plans were regenerated using the Eclipse Treatment Planning System (TPS) (Varian Medical Systems, Palo Alto, CA, USA; Eclipse Version 16) at Moi Teaching and Referral Hospital, Eldoret, Kenya, with a 2 Gy dose per fraction following clinical protocols. The dosimetric impact of anatomical changes was evaluated by comparing the initial treatment plan based on the pCT to the replan on the rCT. The DVH was used to evaluate the two plans by comparing the dose per fraction received by the tumor volume (TV) and organs at risk (OAR). The replan was taken through further review to manually revise the contours made by the TPS upon image registration to give the adapted plan contours. The three plan parameters were copied to be evaluated using the DVH to collect the plan parameters on the target volume data that is the CTV, and its parameters of (maximum dose, minimum dose and mean dose), mean dose to the organs at risk (oral cavity, left parotid gland and right parotid gland) and the plan quality indices (conformity index, heterogeneity index, 3D gamma pass-rate and dose gradient measure). The data was fed in an excel file showing different dose optimization parameters including: 3D gamma pass rate, D_{max}, D_{min}, D_{mean}, conformity index, homogeneity index and TV and OAR (oral cavity and parotid glands) mean dose. Plan 1(original plan) parameters had a one (1) indicated besides the respective parameter's column headers while plan 2 (unadapted plan) and adapted plan (plan 3) had 2 and 3 respectively indicated beside the respective parameters.

Sample Sizes, Statistical Considerations and Synthetic Data Generation

Due to the limited availability of ART datasets, synthetic feature-space augmentation was implemented to improve neural-network training stability under small-sample conditions. The Synthetic Data Generative Model - Variational Autoencoder (SDGM-VAE) was implemented in Python using TensorFlow/Keras as a probabilistic encoder-decoder architecture that learned latent-space representations from TPS-derived dosimetric and volumetric feature vectors extracted from the real patient data. The decoder generated statistically plausible synthetic feature vectors that preserved the general distributional characteristics of the original dataset. 108 synthetic TPS-derived feature-space samples size was selected empirically to improve optimization stability, support gradient-descent convergence and reduce sensitivity to the limited real patient dataset. Synthetic samples were used exclusively for feature-space augmentation and not interpreted as biologically independent patient observations.

Conditional Tabular Generative Adversarial Networks (CTGAN), implemented using the Synthetic Data Vault (SDV) Python library, were used to model the conditional probability distributions of TPS-derived tabular ART features (continuous and categorical). The CTGAN architecture consisted of a generator $G(z,c)$ that synthesized feature vectors from latent noise, z, and condition, c, enabling the learning of statistically plausible dosimetric and volumetric parameter

relationships from the original patient cohort. Following training, CTGAN generated synthetic TPS-derived feature-space samples from plan 1, 2 and 3 parameter distributions to augment APE-Net training. These generated samples represented synthetic tabular feature vectors rather than independently recalculated TPS treatment plans or physical dose distributions.

Training and Validation Procedure for APE-Net (Anatomy-Preserving Estimation Network)

Design and development of the APE-Net framework are illustrated in Figure 1 implemented as a MLP designed to model nonlinear relationships between TPS-derived plans 1 and 2 feature vectors and the corresponding plan 3 adaptive treatment parameters. 1D dosimetric, volumetric and treatment-plan quality scalar features extracted from CT simulation and CBCT-guided adaptive replanning workflows were used. For each real and synthetic TPS-derived feature-space sample, concatenated plan 1 and 2 parameter vectors formed the network input. The corresponding TPS-generated plan 3 parameter vectors served as supervised target outputs._APE-Net learned statistical relationships between original-plan, recalculated-plan and adapted-plan parameter distributions rather than directly performing physical TPS dose recalculation.

To minimize data leakage, patient-level dataset partitioning was performed before augmentation and model training. Synthetic TPS-derived feature-space samples generated using CTGAN and SDGM-VAE were incorporated exclusively into the training subset. Validation and testing were performed only on unseen real-patient TPS-derived feature vectors isolated from augmentation and optimization processes. During validation, only plan 1 and plan 2 feature vectors were provided to the trained model, which predicted the corresponding plan 3 parameters.

APE-Net architecture consisted of an input layer followed by three fully connected dense hidden layers of 128, 64 and 32 neurons respectively with Rectified Linear Unit (ReLU) activation functions. A dropout rate of 0.2 was introduced between hidden layers during training. This was to limit excessive parameter fitting and improve generalization stability. The framework was implemented in Python using Keras deep-learning interface with a TensorFlow computational backend. Prior to model training, TPS-derived feature vectors were normalized and standardized using scikit-learn.

The optimization of the model was performed through grid-search evaluation of multiple training configurations. These included batch sizes (16, 32, 64), learning rates (0.1, 0.01, 0.001), dropout ranges (0.1–0.5), epoch intervals (20–100) and hidden-layer structures. The final selected configuration was trained for 30 epochs with a batch size of 32 and the Adam optimization algorithm with an initial learning rate of 0.001. Mean squared error (MSE) was used as the objective loss function for minimizing differences between predicted adaptive outputs and TPS-derived target parameters. Training and validation loss profiles were monitored throughout optimization to evaluate convergence behavior and generalization trends. Validation performance was evaluated using coefficient of determination (R^2), mean absolute error (MAE) and root mean squared error (RMSE).

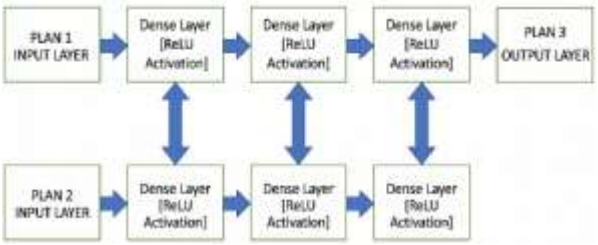

Figure 1. Schematic of APE-Net Model.

Results

Training and validation loss curves were monitored across epochs to evaluate model performance and generalization. The learning pattern of APE-Net in estimating plan 3 parameters is shown in Figure 2. The progressive decline in MSE over 32 epochs during training, indicating effective feature learning and optimization convergence were demonstrated in the training loss and validation loss. Although the validation loss remained consistently higher than the training loss, no severe divergence between the curves was observed across epochs. This meant controlled optimization pattern with limited evidence of marked overfitting. The model achieved a R^2 of 0.681, indicating moderate predictive agreement between predicted and TPS-derived adaptive parameters. The MAE of 9.092% and RMSE of 16.776% indicated the presence of moderate prediction error and occasional higher-magnitude deviations within certain adaptive cases.

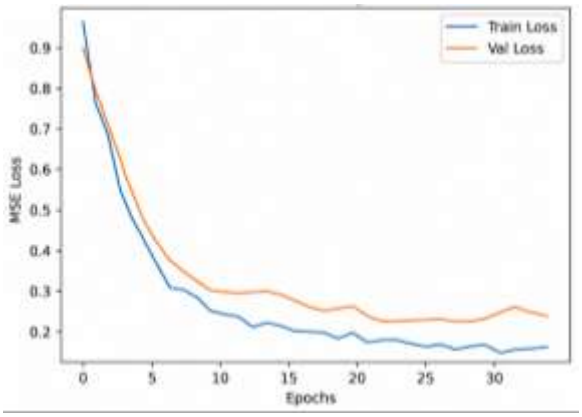

Figure 2. Illustration Curve of APE-Net Training and Validation.

Correlating Actual vs Predicted Results

The scatter plots for the clinical target volume (CTV) of the adapted plan were shown in Figure 3. Predicted values for CTV_3 followed the ideal line, y = x, across the observed range (~300–1000). The majority of data points were concentrated within a narrow margin of the reference line,

especially within the lower to mid-range (~300–600). At higher values (>600), an increase in dispersion was observed, with deviating above the ideal line. The relationship between predicted and actual values for $GRAD_3$ is shown in Figure 4. Predicted values for $GRAD_3$ aligned with the ideal line over the range of approximately ~2.0–5.5. Most of the data points were located close to the ideal line, with limited dispersion across the full range. The spread remained relatively uniform from lower (~2.0–3.0) to higher values (~4.0–5.5), with minor deviations observed both above and below the ideal line.

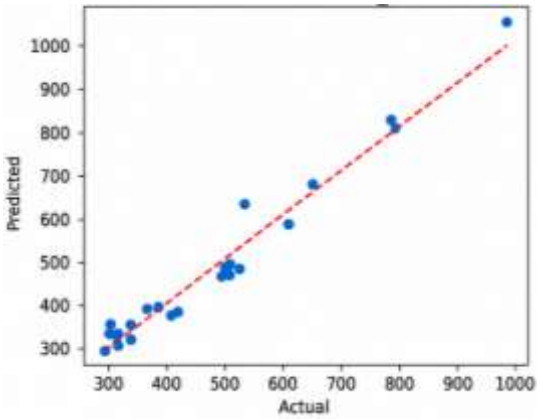

Figure 3. Illustration of predicted values of CTV_3.

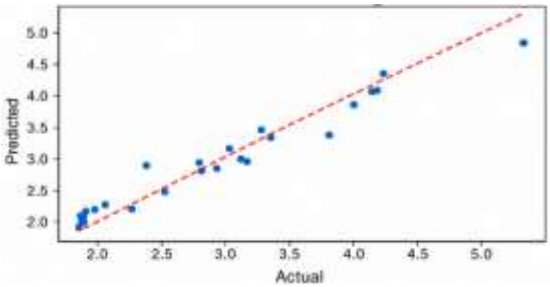

Figure 4. Illustration of predicted values of $GRAD_3$.

The relationship between predicted and actual values for $GAMMA_3$ is shown in Figure 5. Most predictions clustered around 98–100, which indicated a compressed output range relative to the actual values (96–104). At lower values (~96–97), the model overestimated while there was underestimation in the higher values (~102–104), with deviations of up to ±3 - 4 units. This suggests the model captured the central tendency (~99–100) but showed reduced sensitivity to variability, reflecting regression towards the mean.

Figure 6 illustrates that the predicted HI_3 and the actual values had close agreement (~0.25 – 1.25). Most predicted values remained near the ideal line with comparatively limited dispersion relative to several other evaluated parameters. There was slight overestimation observation at lower HI_3 values (~0.25–0.40), while slight underestimation appeared in the upper range (~1.00–1.25). Predictions within the intermediate interval (~0.60–0.90) remained more consistently aligned with the TPS-derived values. These observations suggest that the framework captured general HI_3 variation with comparatively improved stability across the evaluated parameter range.

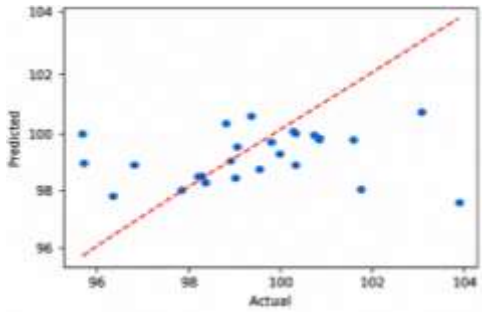

Figure 5. Illustration of Predicted Values of the $GAMMA_3$.

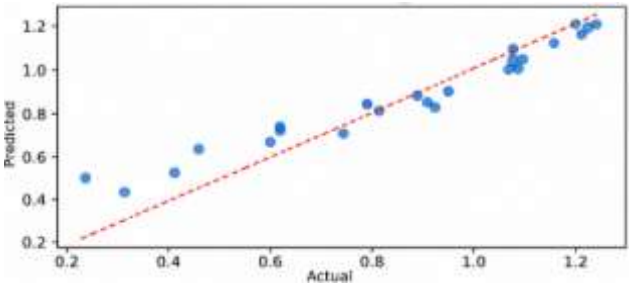

Figure 6. Illustration of Predicted Values of the Adapted HI_3.

Discussion

Figure 2 showed progressive reduction in both training and validation MSE during optimization. This indicated continued parameter learning across the training epochs [9] [10]. The validation loss remained slightly higher than the training loss throughout optimization, but there was no marked divergence between the curves observed [11]. This suggests that the model maintained controlled optimization trend with limited evidence of severe memorization of training patterns despite the restricted dataset size [12]. Such behavior is important for predictive-support frameworks intended for adaptive radiotherapy workflows involving previously unseen patient data.

The achieved coefficient of determination (R^2 = 0.681) indicates moderate agreement between predicted and TPS-derived adaptive parameters, although a considerable proportion of adaptive variance remained unexplained [13]. The MAE (9.092%) and RMSE (16.776%) further demonstrate the presence of moderate prediction error, with the larger RMSE reflecting occasional higher-magnitude deviations within certain adaptive cases [14]. Consequently, the framework is more appropriately interpreted as a TPS-informed predictive screening and triage-support system for offline adaptive radiotherapy rather than as a replacement for TPS-based adaptive dose recalculation or independent clinical replanning [15].

Parameter-specific evaluation showed that predicted CTV_3 values remained close to the ideal line within the

lower to mid-range (~300–600), where most treatment samples were concentrated [16]. As the target volume (TV) increased > 600, wider dispersion became more apparent. This indicates less stable estimation behavior for larger adaptive cases [17]. This may reflect increased anatomical variability together with limited representation of extreme TV patterns within the training dataset [17]. $GRAD_3$ values showed nearly smaller dispersion across the evaluated range (~2.0–5.5), with predictions remaining distributed near the ideal line. The framework therefore appeared capable of reproducing general gradient-related dosimetric trends with relatively consistent behavior across varying parameter values [18]. Compared to CTV_3, $GRAD_3$ demonstrates less sensitivity to variability at higher values.

For $GAMMA_3$, the predicted outputs were concentrated within a narrower interval (~98–100) despite the broader TPS-derived range (~96–104). Lower observed values (~96–97) tended to be overestimated. Larger values (~102–104) were underestimated, with deviations approaching ±3–4 units near the extremes. This compression toward the central range reflects regression toward the mean behavior and reduced sensitivity to pronounced adaptive variation [19]. Clinically, this represents an important limitation because patients with substantial anatomical and dosimetric changes are often those most likely to require ART intervention [20]. Although APE-Net reproduced general adaptive dosimetric patterns, reduced responsiveness to outlier cases limits its suitability for independent ART and high-precision clinical decision-making [21]. Consequently, the framework is more appropriately interpreted as a TPS-informed predictive screening and triage-support system for oART workflows [22]. HI_3 predictions showed comparatively closer agreement with TPS-derived values across the evaluated range (~0.25–1.25). Most data points remained near the ideal line. Slight overestimation was observed at lower HI_3 values, whereas slight underestimation became more apparent toward the upper range (~1.00–1.25) [23]. Compared with $GAMMA_3$ and CTV_3, the HI_3 distribution demonstrated lower dispersion and more stable alignment across intermediate values. The comparatively improved HI_3 pattern may relate to its broader dynamic range and smoother parameter variation. This likely improved feature discrimination during optimization [24]. The narrower $GAMMA_3$ distribution restricted variability between neighboring values and reduced predictive sensitivity near the distribution extremes [24].

Conclusion

This study developed and evaluated APE-Net as a TPS-informed ML assisted predictive support framework for supporting oART in HNC using 21 real patient cases and 108 synthetic TPS-derived feature-space samples. The framework demonstrated moderate capability in estimating adaptive dosimetric parameters (CTV_3, $GRAD_3$) and treatment quality indices($GAMMA_3$, HI_3), although reduced sensitivity to extreme adaptive variations remained an important limitation. The findings support the feasibility of integrating TPS-informed predictive modelling and CBCT-guided adaptive assessment into oART support workflows in resource-constrained settings as a decision making or early predictive frameworks. Although it needs detailed work to replace TPS-based adaptive replanning, APE-Net may assist in preliminary predictive screening, patient triage and adaptive workflow prioritization. Further validation using larger real-patient datasets and spatially resolved learning approaches is required before independent clinical implementation.

Acknowledgment

This article is an excerpt from an MSc thesis by Daniel Ndegwa, and was also approved by the Moi Teaching and Referral Hospital/Moi University Institutional Scientific and Ethical Review Committee (MTRH/MU-ISERC) under approval number 0005091 and Chuka University Institutional Ethics Review Committee (CUIERC) under reference number CUIERC/NACOSTI/830. Research authorization was further granted by the National Commission for Science, Technology and Innovation (NACOSTI), Kenya, under research license number NACOSTI/P/25/4177302 and reference number 355200. This research received support from Department of Physical Sciences, Chuka University and Radiotherapy Department at Moi Teaching and Referral Hospital, Kenya in providing high performing computers for computations, modelling and data analysis. A special mention to my mum, Jenifer, and my siblings for their financial and moral support during my research period.

References

1. Elizaveta Lavrova, Garrett MD, Wang Y, Chin C, Elliston CD, Savacool M, et al. Adaptive Radiation Therapy: A Review of CT-based Techniques. Radiology. 2023 Jul 1;5(4).
2. Morgan HE, Sher DJ. Adaptive radiotherapy for head and neck cancer. Cancers of the Head & Neck. 2020 Jan 9;5(1).
3. Maja Guberina, Nika Guberina, Hoffmann C, A. Gogishvili, Freisleben F, Herz A, et al. Prospects for online adaptive radiation therapy (ART) for head and neck cancer. Radiation oncology. 2024 Jan 8;19(1).
4. Zafar F, Vilsan J, Mani S, Al AR, Cano-Reyes SE, Abraham G, et al. AI in radiation oncology: a comprehensive review of current applications and future directions. Cureus [Internet]. 2025 Sep 22 [cited 2025 Sep 23];17(9):e398228.
5. Blumenfeld PA, Feldman J, Arbit E, Weizman N, Berger A, Hillman Y, et al. Daily Artificial Intelligence-Assisted Adaptive Radiotherapy on Cone-Beam CT for Cancer of the Head and Neck. International Journal of Radiation Oncology*Biology*Physics. 2022 Oct 22;114(3):e590–1.

6. Liu H, Schaal DW, Curry H, Clark R, Magliari A, Kupelian PA, et al. Review of cone beam computed tomography based online adaptive radiotherapy: current trend and future direction. Radiation Oncology. 2023 Sep 2;18(1).
7. Glide-Hurst CK, Lee P, Yock AD, Olsen JR, Cao M, Siddiqui F, et al. Adaptive Radiation Therapy (ART) Strategies and Technical Considerations: A State of the ART Review From NRG Oncology. International Journal of Radiation Oncology*Biology*Physics. 2021 Mar;109(4):1054–75.
8. Chen L, Sun H, Wang Z, Zhang T, Zhang H, Wang W, et al. Deep learning architecture with shunted transformer and 3D deformable convolution for voxel-level dose prediction of head and neck tumors. Physical and Engineering Sciences in Medicine. 2024 Aug 5;47(4):1501–12.
9. Subramanian S. Training and Inference Time Dynamics of Artificial Neural Networks. Artificial Intelligence. 2025 Nov 14.
10. Temmar H, Willsey MS, Costello JT, Mender MJ, Cubillos LH, DeMatteo JC, et al. Investigating the benefits of artificial neural networks over linear approaches to BMI decoding. J Neural Eng [Internet]. 2025 Jun 17 [cited 2025 Sep 20];22(3):036012.
11. Wang L, Jiang J, Ghita O, Zhu Y, Sucala VI. Knowledge-enabled stress–strain prediction in additive manufacturing via transferable deep temporal modelling. Advanced Engineering Informatics. 2026 Jan;69:104004.
12. Montesinos López OA, Montesinos López A, Crossa J. Overfitting, model tuning, and evaluation of prediction performance. In: Multivariate statistical machine learning methods for genomic prediction [Internet]. Springer; 2022. p. 109–139.
13. Shaban OS, Omoush A. AI-Driven Financial Transparency and Corporate Governance: Enhancing Accounting Practices with Evidence from Jordan. Sustainability. 2025 Apr 23;17(9):3818.
14. Chai T, Draxler RR. Root mean square error (RMSE) or mean absolute error (MAE)? – Arguments against avoiding RMSE in the literature. Geoscientific Model Development. 2014 Jun 30;7(3):1247–50.
15. Vandewinckele L, Claessens M, Dinkla A, Brouwer C, Crijns W, Verellen D, et al. Overview of artificial intelligence-based applications in radiotherapy: Recommendations for implementation and quality assurance. Radiotherapy and Oncology [Internet]. 2020 Dec 1;153:55–66.
16. Song B, Jiang G, Liu Y, Cheng D. A clinical prediction model for central venous catheter-associated bloodstream infections: derivation and validation from the MIMIC-IV cohort. European Journal of Medical Research. 2026 Jan 6;31(1).
17. Guzman-Pando A, Enriquez-Guillen BO, Ramirez-Alonso G, Camarillo-Cisneros J, Aguilar-Torres CR, Hinojos-Gallardo LC. AI-FRS: An Ensemble-Based AI Decision-Support System for Fetal Risk Prediction in a Mexican Clinical Setting. AI. 2026 Apr 1;7(4):129.
18. Zhang Z, Zhao Y, Canes A, Steinberg D, Lyashevska O. Predictive analytics with gradient boosting in clinical medicine. Annals of Translational Medicine. 2019 Apr;7(7):152–2.
19. Emanuel KS, Dahmen J, Sierevelt IN, Mats Brittberg, Kerkhoffs GMMJ. Regression to the Mean: Statistical Bias Can Mislead Interpretation in Cartilage and Osteoarthritis Clinics and Research. Cartilage. 2024 Nov 11.
20. Suwanraksa C, Sukcharoen W, Phuakphiuwong S, Kooptisirirat S, Krutsuwan K, Nantasri C, et al. Time series analysis of dosimetric changes in target volumes and organs at risk monitored by cone beam computed tomography during radiotherapy for non-small-cell lung cancer. Physics and Imaging in Radiation Oncology. 2025 Jul;35:100822.
21. Wang YW, Chen M, Shen WT, Xu HP. The clinical practice and dosimetric outcome of the manual adaptive planning during definitive radiotherapy for cervical cancer. Journal of Cancer Research and Clinical Oncology. 2024 May 27;150(5):280–0.
22. Hanieh Alimiri Dehbaghi, Karim Khoshgard. Revolutionizing emergency care: an overview of the transformative role of artificial intelligence in diagnosis, triage, and patient management. International Journal of Emergency Medicine. 2025 Nov 17;18(1):242–2.
23. Luijken K, Song J, Groenwold RHH. Quantitative prediction error analysis to investigate predictive performance under predictor measurement heterogeneity at model implementation. Diagn Progn Res. 2022 Apr 7 [cited 2024 Feb 24];6(1):8.
24. Liu Y, Tian Y, Wang S, Zhang X, Kwong S. Overview of High-Dynamic-Range Image Quality Assessment. Journal of Imaging. 2024 Sep 27;10(10):243.